FULL PAPER

White Light-Emitting Diode From Sb-Doped p-ZnO Nanowire Arrays/n-GaN Film

*Xiaoliang Ren, Xianghui Zhang, Nishuang Liu, Li Wen, Longwei Ding, Zongwei Ma, Jun Su, Luying Li, Junbo Han, and Yihua Gao**

A whole interfacial transition of electrons from conduction bands of n-type material to the acceptor levels of p-type material makes the energy band engineering successful. It tunes intrinsic ZnO UV emission to UV-free and warm white light-emitting diode (W-LED) emission with color coordinates around (0.418, 0.429) at the bias of 8–15.5 V. The W-LED is fabricated based on antimony (Sb) doped p-ZnO nanowire arrays/Si doped n-GaN film heterojunction structure through one-step chemical vapor deposition with quenching process. Element analysis shows that the doping concentration of Sb is ≈1.0%. The *I–V* test exhibits the formation of p-type ZnO nanowires, and the temperature-dependent photoluminescence measurement down to 4.65 K confirms the formation of deep levels and shallow acceptor levels after Sb-doping. The intrinsic UV emission of ZnO at room temperature is cut off in electroluminescence emission at a bias of 4–15.5 V. The UV-free and warm W-LED have great potential application in green lights program, especially in eye-protected lamp and display since television, computer, smart phone, and mobile digital equipment are widely and heavily used in modern human life, as more than 3000 h per year.

1. Introduction

Although the first practical red light-emitting diode (LED) was developed as early as 1962,[1] the desire for low power consumption and long-lifetime solid-state white light-emitting diodes (W-LEDs) with high light efficiency is still a challenge of replacing low-lifetime traditional lighting with high electric energy consumption.[2–4] Usually, the realization of white-LEDs requires reliable monochromatic light technology for blue and green LEDs based on nitride semiconductors, which has been quite mature in three general approaches.[2,5] However, some problems still exist. First, the direct mixing of three monochromatic sources, i.e., red, green, and blue (RGB) to generate a sensuous white light, has problems of ineffective control, high cost, and heat dissipation.[6] The second technique using an UV-LED to pump RGB hybrid phosphors to achieve white light has low efficiency and mismatched phosphor synthesis hindering the practical lifetime of the lamp.[7] The third method, the phosphor-converted W-LED occupying the major LED illumination markets by far, which consists of a blue LED pumping a complimentary yellow phosphor, has also inherent less efficiency.[8] In addition, a burgeoning technology of organic light-emitting diodes (OLEDs) based W-LEDs is developing and needs multiple and stable organic materials.[9–11] All of these methods are of technical sophistication and unsatisfactory practicability.

With the explosion of information and internet technologies, computer, smart phone, mobile digital terminals, and television are playing more and more important roles in modern life. Multitudes of people must stay focus on looking the LED-backlight display for more than 10 h one day and 3000 h one year. As we know, the LED backlight spectrum contains not only useful visible light but also blue light even UV light, which could hurt human eyes seriously after long time irradiation. The comfortable and harmless W-LED for reading should emit UV-free and warm white light. In order to realize one pace reach of UV-free and warm white light, excellent materials with simple structure based on suitably wide bandgap engineering are needed. ZnO and GaN are such materials (their intrinsic bandgaps 3.37 and 3.39 eV at room temperature (RT)), which could be tuned into visible range in theory.[12] However, it is hard to directly tune bandgap on GaN and/or ZnO films for UV-free and warm W-LEDs.

On comparison with traditional thin film structure, doping on one-dimensional (1D) vertical nanowire (NW) arrays is an effective approach to bandgap tuning because of the dispersed geometry and high surface areas, which can offer easy element doping, release their lattice strains between doping element and matrix, NWs and substrate.[13] However, it is very difficult

X. Ren, Dr. X. Zhang, Dr. N. Liu, L. Wen, L. Ding, Dr. J. Su, Dr. L. Li, Prof. Y. Gao
Center for Nanoscale Characterization & Devices (CNCD)
Wuhan National Laboratory for Optoelectronics (WNLO)-School of Physics
Huazhong University of Science and Technology (HUST)
LuoyuRoad 1037, Wuhan 430074, P.R. China
E-mail: gaoyihua@hust.edu.cn
Dr. X. Zhang, Prof. Y. Gao
Hubei Collaborative Innovation Center for Advanced Organic Chemical Materials
Faculty of Physics & Electronic Science
Hubei University
Wuhan 430062, P.R. China
Z. Ma, Dr. J. Han
Wuhan National High Magnetic Field Center
HUST, Luoyu Road 1037, Wuhan 430074, P.R. China

DOI: 10.1002/adfm.201404316

to obtain GaN NW arrays by a direct growth until now, and no bandgap engineering W-LEDs of ZnO based nanowire homojunctions were successful. On the other hand, heterojunction LED of ZnO based nanowires may work as a W-LEDs. Since GaN has the same wurtzite hexagonal structure, the tiny lattice mismatch of 1.86% in direction *a* and 3.45% in direction *c*, and the similar crystalline properties as ZnO, GaN is thus considered as a good epitaxial substrate for ZnO NW devices. Therefore W-LED may be realized in the transition processes that electrons in the conduction band of n-type material (one of GaN and ZnO) recombine with the holes in the acceptor energy level introduced in the forbidden band of p-type material (the other of GaN and ZnO). N-type ZnO NW arrays grown on p-type GaN substrate LED devices have been studied in the past several years,[14–18] but violet–blue emissions dominated the LED devices owing to the intrinsic direct emission related to band edges of ZnO and GaN and the absence of deep level emissions. Recently, we also tuned the bandgap by Ga alloying doped ZnO NW arrays LED on p-GaN substrate,[13] but the larger redshift is only 98 nm, from 380 to 478 nm in the RT electroluminance (EL) emission.

Direct bandgap engineering W-LEDs may be realized by p-type doping ZnO nanowire/n-GaN substrate, and thus a powerful p-type doping is necessary. Sb-doping is such a candidate among many p-type doping approaches using nitrogen, phosphorus, and magnesium etc. Several years ago, Limpijumnong et al. predicted the possibility of forming p-type ZnO by large-size-mismatched impurity Sb-doping through first-principles calculations using Sb_{Zn}–$2V_{Zn}$ complexes model.[19] Chu et al. first demonstrated the 390 nm ZnO NW diode RT laser with electrical pumping using Sb-doped p-type ZnO nanowires and n-type ZnO film.[20] Recently, Sb-doped p-type ZnO nanowires were confirmed tightly.[21–23] Based on these studies, can we go further by using p-type Sb doped ZnO NWs on n-type GaN substrate for white LED?

2. Results and Discussion

The LED approach of Sb-doping ZnO nanowire/n-GaN substrate is shown in **Figure 1**a, where indium and indium-gold thin films are used for the two electrodes, and the n-type doped GaN was grown on sapphire. Figure 1b gives the model of a Sb atom substituting a Zn atom by chance, where the Zn atoms are equal at all sites. In Figure 1c, the recombination energy between electrons and holes is determined by the CB offset ΔE_c between the two conduction bands (CBs) of ZnO and GaN if a whole interfacial transition occurs between GaN and ZnO. The offset ΔE_c is tuned by ΔV_f, the voltage difference imposing on the interface emission area, which may increase with the forward bias voltage V of the whole device but is much less than V because only a small part of V is imposed on the interface.[15]

Figure 2a presents the oblique-view scanning electronic microscope (SEM) image of large-area ZnO:Sb NWs, which shows good uniformity and consistency, and the length and diameter of the nanowires are on average 5 μm and 40 nm, respectively. For comparison, the x-ray diffraction (XRD) patterns of pure ZnO and Sb-doped ZnO nanowires were carried out (Figure 2b),[16,20] which showed good crystallinity with clearly ZnO (002) and (004) peaks, even the Sb atoms have relatively bigger size than Zn.[24] A full-elements X-ray photoelectron spectrum (XPS) analysis of ZnO:Sb NWs shows clear evidence of Sb (Figure S2a, Supporting Information). Figure 2c gives more accurate binding energies of Sb. The peak located

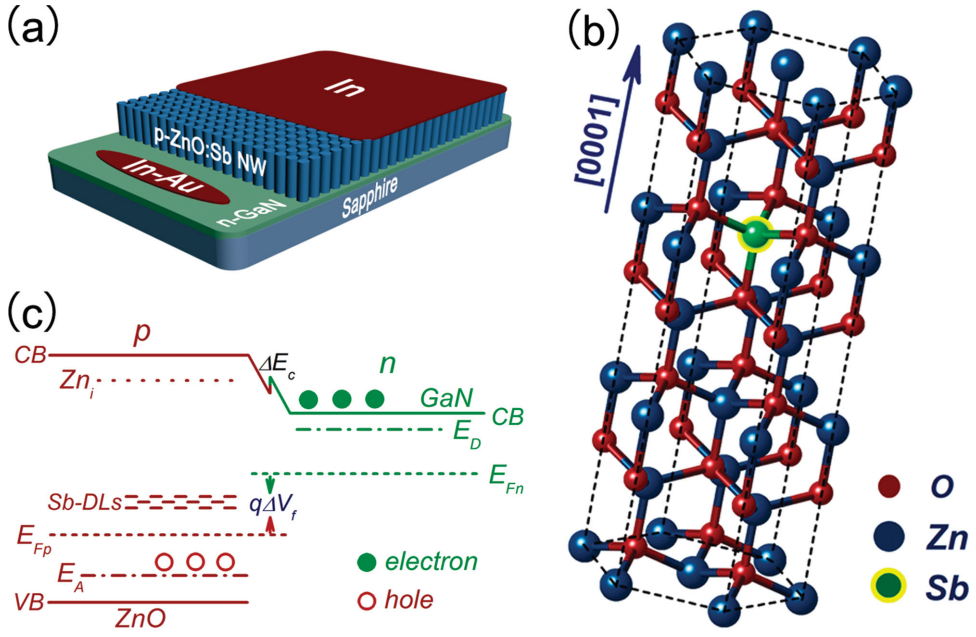

Figure 1. The LED approach of Sb-doping ZnO nanowire/n-GaN substrate. a) Schematic of the heterojunction LED. b) A Zn atom in ZnO lattice is replaced by a Sb atom. c) White light may be obtained by a whole interfacial transition, where the electrons from the CB of n-type GaN recombine the holes from the deep acceptor levels in p-ZnO. The violet–blue intrinsic emission may occur after the imposed voltage ΔV_f on the interfacial region is big enough, which decrease the CB offset ΔE_c and upgrade the CB of GaN to a level higher than the level of Zn_i and even the CB of ZnO.

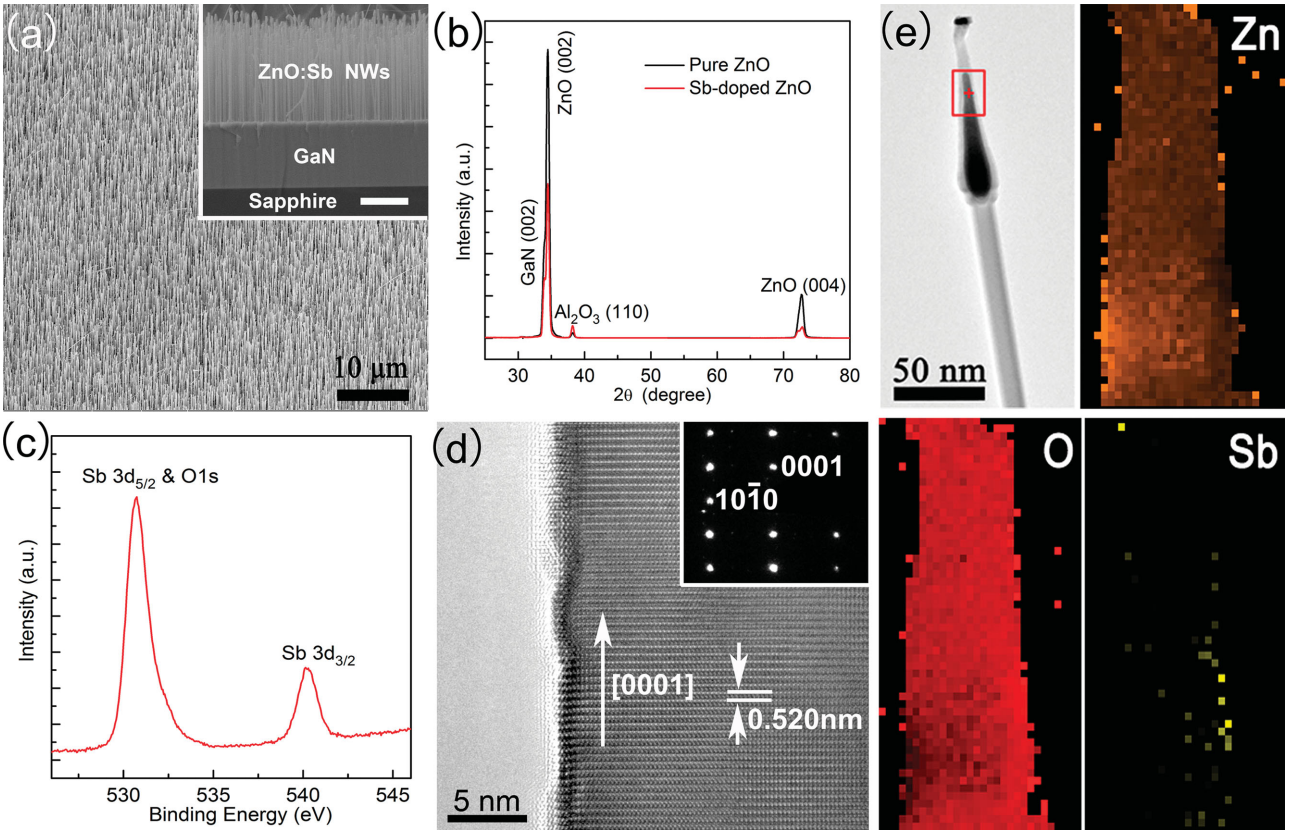

Figure 2. Structure and characterization of the Sb-doped ZnO NWs. a) Large area 30° oblique-view SEM image of ZnO:Sb NWs. The inset SEM image shows the p-n heterointerface of the NW arrays on GaN film, scale bar 5 μm. b) XRD comparison of the ZnO:Sb NWs/n-GaN film and pure ZnO NWs/n-GaN film based on sapphire. c) Precise narrow XPS scanning of the inner Sb-3d orbital electrons. d) The HRTEM image shows that the Sb-doping ZnO NWs are well crystallized. The 0001 diffraction should be a forbidden one in ideal ZnO, but it is very strong here due to two reasons, one is that the ZnO is thick and the second diffraction between the (10$\bar{1}$0) and (10$\bar{1}$1) diffractions, the other is that Sb doping destroys the symmetry. e) The morphology of a single ZnO:Sb nanowire with a Au tip as catalyst with elemental mapping of the Zn (orange), O (red), and Sb (yellow).

at 530.7 eV should be attributed to the superposition of Sb 3d5/2 and O 1s peak, which increased the difficulty of the accurate calculation of Sb content.[25] However, we obtained the Sb 3d3/2 peak at 540.2 eV, which could be induced by the formation of Sb_{Zn}–$2V_{Zn}$ complexes, since the standard Sb 3d3/2 peak of Sb and Sb_2O_3 is 518.7 and 539.6 eV,[26,27] respectively. The shift of Sb 3d3/2 peak also suggested that Sb atoms have been doped into ZnO and substituted Zn atoms.[25,28] An obvious deviation from 766.4 eV of pure Sb to 768.7 eV of Sb in ZnO was observed at the inner 3p3/2 orbital electrons (Figure S2b, Supporting Information). A ≈0.1 eV difference of 2p binding energy of Zn in Sb:ZnO smaller than that of Zn in ZnO is also observed and may be due to the Sb_{Zn}–$2V_{Zn}$ complexes and p-type doping (Figure S2c, Supporting Information).

High-resolution transmission electron microscopy (HRTEM) image of an individual ZnO:Sb nanowire is shown in Figure 2d. Lattice with 0.520 nm spacing (two times of $(0002)_{ZnO}$ lattice spacing) is clearly seen, and the inset shows the corresponding selected area electron diffraction (SAED) pattern, which shows good single crystalline with wurtzite nature of the nanowire grown along a preferentially *c*-axis after Sb doping. Figure 2e shows the energy dispersive X-ray spectroscopy (EDS) elemental mapping of Zn, O, and Sb from the single ZnO:Sb NW. Figures S3 and S4, Supporting Information, show the EDS mapping of Au, Zn, O, and Sb elements of the tip of a single ZnO:Sb NW and some ZnO:Sb NWs, respectively. Through the above analysis, we can conclude that the well crystallized ZnO nanowire arrays were doped by Sb successfully using one-step chemical vapor deposition (CVD) method. By using an EDS of ZnO:Sb NWs, we can estimate the Sb atom ratio as ≈1.0% (Figure S5, Supporting Information).

We test a normalized RT photoluminance (PL) spectrum for the GaN film, undoped ZnO, and Sb-doped ZnO NWs (**Figure 3**a). For n-GaN and undoped ZnO, typical eigenvalues of 3.418 and 3.266 eV were characterized, respectively. But for Sb-doped ZnO, the intrinsic emission is at 3.220 eV, with a marked deviation of 0.040 eV from the emission (3.266 eV) of undoped ZnO, or 0.150 eV from the bandgap (3.37) eV of ZnO, which is probably due to the formation of acceptor levels by Sb doping. Meanwhile, in the long wavelength region, we clearly see the increased emission that should be induced by Sb doping,[22,25] which provides more abundant light emission levels centered at 2.38 eV (521 nm, green), as also shown in Figure S6, Supporting Information.

We carried out steady-state PL measurements in the temperature range from 4.65 to 300 K using a 344 nm Ti: sapphire laser with an excitation power of 0.5 mW (Figure 3b). At low temperatures, emission with excitons bound to neutral donors

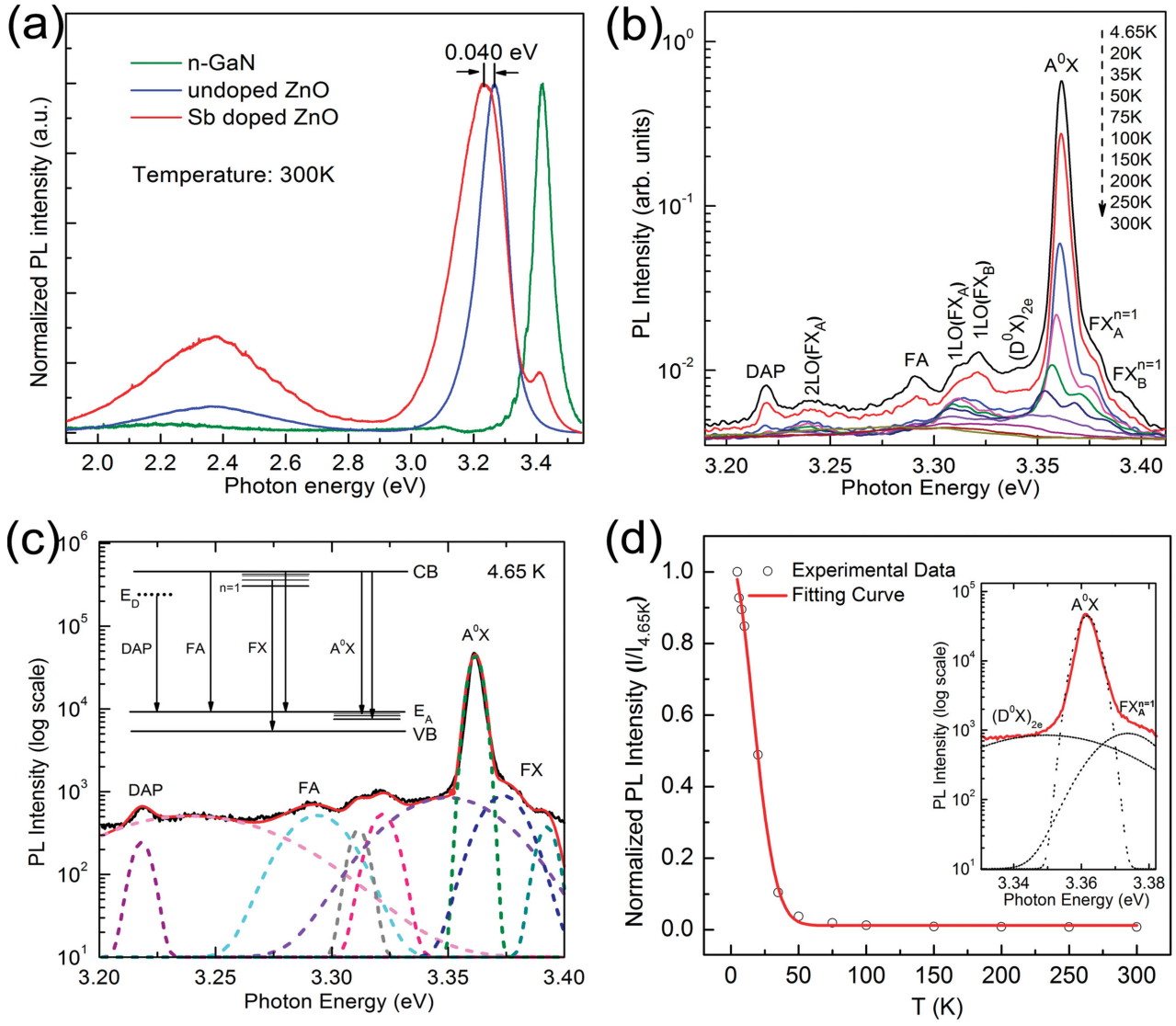

Figure 3. Temperature-dependent PL spectra characterization of p-ZnO:Sb NWs. a) Normalized PL spectra comparison of pure ZnO and p-ZnO:Sb NWs at RT. b) Temperature-dependent PL spectra from 4.65 to 300 K. c) Multipeaks fitting of PL spectra of Sb-doped ZnO NW arrays at $T = 4.65$ K, the inset shows the corresponding schematic of energy levels. d) The normalized intensity of the A_0X emission as a function of temperature. The inset shows the spectrum ($T = 4.65$ K, p-ZnO:Sb NWs, red line) analyzed by using a multiGaussian fitting.

or acceptors was the dominant radiative channel, but free exciton emission usually took over at higher temperatures. The specific peaks DAP, FA, $(D^0X)_{2e}$, FX, A_0X confirmed the p-type behavior of the ZnO:Sb NWs, which are discussed in Figure S7, Supporting Information. It is obvious that the A^0X peak shifts to red side with temperature increase.

Figure 3c shows the near band edge (NBE) PL emission spectrum of Sb-doped ZnO nanowires at 4.65 K. Abundant valence band edge information can be well fitted by nine Gaussian peaks. The inset showed the corresponding schematic diagram of energy level emission. It appears that the emission related to the acceptor level plays a leading role, which further suggested the formation of stable and reliable acceptor levels. It should be mentioned that some other energy levels of point defects may also exist in ZnO lattice such as V_O (vacancies of O atoms) and Zn_i (interstitial Zn atoms) as donors, V_{Zn} (vacancies of Zn atoms) and O_i (interstitial O atoms) as acceptors, which has been elaborated by many theoretical calculations and experimental results.[29] Although they are not the main emission in PL spectrum, they may play a role in our LED at RT. Meanwhile, it was worthy noting that p-ZnO formed by doping still retained weak donor level and played supporting role, which was well indicated by peak-fitting. Figure 3d gives the normalized temperature-dependent A^0X emission,[24] in which we can get the acceptor binding energy E_A as 0.139 eV using the data of Figure 3c,d (see the theoretical analysis in the Supporting Information).

An *I–V* examination of the heterojunction Sb:ZnO/GaN diode structure was shown in **Figure 4**a, which indicated an obvious p-n diode rectification behavior with a forward bias

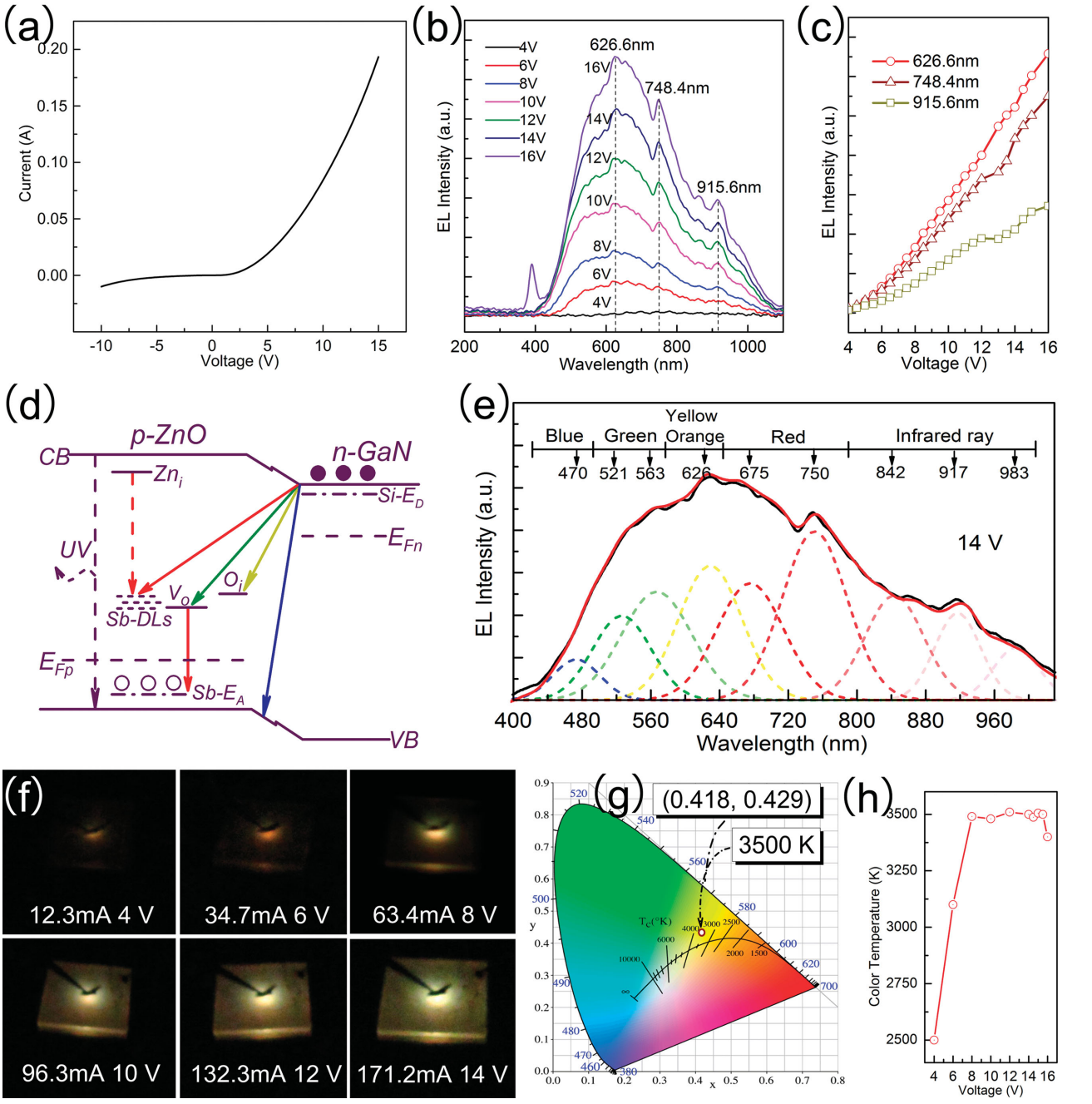

Figure 4. Characterization of the warm white LEDs device. a) *I–V* characteristics of the p-n heterojunction LED at RT. b) Voltage-dependent EL spectra of the device. c) The EL intensity of three obvious EL peaks with voltage. d) Schematic diagram of p-ZnO dominant energy level emission and interface recombination with GaN. e) Gaussian fitting curves of EL spectra at 14 V. f) Photo galleries of room temperature EL emission from p-ZnO/n-GaN LEDs at the forward bias from 4 to 14 V. g) CIE chromaticity diagram of warm white LED with EL spectra at 14 V. h) Voltage-dependent color temperature changes from p-ZnO/n-GaN LEDs.

turn-on voltage of 3.74 V. The heterojunction behaves like an efficient diode with a current increasing rapidly under forward bias and blocking the current flow under reverse bias till –5.0 V. After the continuous increase of reverse bias, the increase of reverse current becomes larger and larger. Many p-n junctions have such a typical characteristic before they are broke down. Since the top ZnO nanoarrays and bottom GaN layer were contacted directly with the In-electrode, and In–Au electrode, respectively, the p-n characteristics is not aroused by the contacts of In electrode and p-ZnO, In–Au electrode and n-GaN film, which have Ohmic characteristic, as shown in Figure S8, Supporting Information. The above analysis indicated that the Sb-doped ZnO nanowires are exactly p-type.

Figure 4b presents the EL spectra of the fresh LED device from 4 to 16 V at RT. The LED emission with threshold of about 4.0 V was studied, which is close to the turn-on voltage (3.74 V)

of the p-n heterojunction. With the applied voltage increase, the 748.4 nm red light and 915.6 nm infrared ray are gradually obvious, and the intensity of the main peak at 626.6 nm (1.98 eV, red) also increase linearly (Figure 4c).

No matter what the ZnO device is based on, the homojunction or heterojunction ZnO, the emission most results from radiative recombination in ZnO band-edge peaks but seldom junction interface transition recombination really works, and both ZnO PL and EL emissions are similar in that a pointed peak always appeared in the violet–blue region.[30] That is, it is relatively easy to realize the ultraviolet emission attributed to ZnO internal energy level transition, while the visible peaks from junction are challenging. In the studies,[14,31] the violet-blue is always observed in undoped ZnO based LEDs, which inhibit the near-UV emission attributed to the NBE and generate shorter wavelength and multispectrum light. In our work, the RT EL is remarkably different from the above studies. No UV light of ZnO or GaN was emitted at bias of 4–15.5 V, which indicates that our UV-free emission must be due to a whole interfacial transition of electrons on a lower CB of n-type GaN to the acceptor levels of p-type ZnO. Otherwise, the UV light should emit. Our RT PL spectrum strongly suggested that more and deep levels were introduced by Sb doping, which affected the deep level emission in ZnO and generated the colors in the visible region in the RT EL.

Typical ZnO related violet-blue emission peak (391 nm, 3.17 eV) was invisible till the imposed voltage of 16 V (Figure S9, Supporting Information). The reason is that a big imposed ΔV_f on the interfacial region is induced by the higher forward bias of 16 V, which may upgrade CB of the GaN to a level higher than the band of Zn_i (E_d = 0.22 eV) in ZnO,[15] then the electrons can be transported to the band of Zn_i, leading to the violet–blue emission (3.37 − 0.22 = 3.15 eV). In a word, only at this high bias voltage, the violet–blue emission peak occurred, which means that the ZnO has lost its own intrinsic band-edge radiative recombination while the visible light emission can occur with a strong intensity. Moreover, we can indicate that the CB offset of ZnO and GaN in the bias of 8–15.5 V is $E_c \approx 0.4$ V by comparing the two wavelength values of the highest intensity peaks (2.38 eV, 1.98 eV) in PL and EL spectra.

Therefore, the UV-free and visible peaks (4–15.5 V bias) should result from the whole recombination in the heterojunction interface of p-ZnO:Sb/n-GaN, where the electrons with energy lower than the CB of ZnO are transported from n-GaN to deep levels and acceptor levels of p-ZnO NWs after Sb-doping. We give a tentative explanation for luminous mechanism based on existing theory in the diagram (Figure 4d). It is believed that electron–hole recombination between CB of GaN and deeply trapped V_O center can explain the green emissions,[32] and the yellow–orange emissions could be attributed to the emission between CB of GaN and O_i like Li dopants in ZnO.[33] Although specific electron transitions are not yet known in detail, the red emissions could be caused the interfacial recombination[13] of electrons of CB in GaN and holes on the deep levels (Sb-DLs) induced by Sb doping. Different from undoped ZnO, stable Sb-DLs could play an important role in red and infrared emission. The weak blue emission is ascribed to the radiative interfacial recombination between the electrons from n-GaN and holes from p-ZnO:Sb assisted by the CB offset.[13,34] The superposition of all emissions generates the white light effect.

Figure 4e gives the EL Gaussian fitting, which show blue, green, yellow–orange, and red peaks approximately centered at 470 nm (2.64 eV, blue), 521 nm (2.38 eV, green), 626 nm (1.98 eV, red), 675 nm (1.84 eV, red), respectively. Figure 4f shows the actual luminous picture, which gives white light intuitively. The more accurate luminous characteristic of white LED (14 V) was analyzed by 1931 Commission Internationale de L'Eclairage (CIE) chromaticity diagram (Figure 4g), which confirmed the formation of warm W-LEDs with chromaticity coordinate of (0.418, 0.429) according to the CIE standard white-light emission (0.33 ± 0.05, 0.33 ± 0.05), and the white light with correlated color temperature (CT) of 3500 K suggests reddish white light.[35] The warm W-LED that gives people stable and warm feeling with promising value is not easy to fulfill by traditional method with one-step. In addition, in the market, the LEDs that can satisfy the requirement of low CT lighting are seldom realized. Interestingly, the CT tending to be stable with applied voltage of 8–15.5 V (Figure 4h) may be owing to the existence of a diffusion capacitance in the heterojunction and the CB of GaN is always unchanged.

3. Conclusion

In summary, we have first demonstrated UV-free and warm white LEDs device based p-ZnO:Sb/n-GaN (NWs/film) heterojunction structure by a whole interfacial transition. The whole interfacial transition emission with CB offset between p-type Sb-doping ZnO and n-type GaN makes the energy band engineering successful, which tunes intrinsic ZnO UV emission to UV-free and warm W-LED emission with color coordinate of around (0.418, 0.429) at the bias of 8–15.5 V. Deep levels and shallow acceptor levels are realized after Sb-doping, thus the intrinsic UV emissions of ZnO at room temperature is restricted in PL emission and cut off in EL emission at a bias of 4–15.5 V. The whole interfacial transition may play an important role in bandgap engineering.

4. Experimental Section

Fabrication of Sb-Doped ZnO NWs on GaN: The p-type ZnO:Sb nanowire arrays grown on commercial n-type Si-doped GaN film with a sapphire base was fabricated by one-step chemical vapor deposition. The n-GaN film is 4 μm-thick, C-axis (0001) oriented on c-plane sapphire (0001) substrate fabricated by MOCVD with carrier concentration of 4.43×10^{17} cm^{-3} at RT. Sb_2O_3 powder (4N) was chosen as antimony doping source. ZnO powder (3N), graphite powder (4N) with a weight ratio of 1:1 ZnO/C and with a molar ratio of 1:1/10 ZnO/ Sb_2O_3 were fully dissolved with ethanol into slurry and baked to powder at 200 °C for 15 min before being loaded in a quartz boat. Before the experiment, the GaN bases were orderly ultrasonicated in acetone at 50 °C for 15 min, in ethanol for 10 min at RT, and in deionized water (Aquapro, 18.25 M Ω cm) for 2 min, repetitiously. Then, the bases were gold plated at 10 Pa vacuum with 2 mA current for 60 s, the thickness of gold catalyst layer was 3–5 nm. The process of chemical vapor deposition (CVD) was carried out using a simple two-heater tube furnace. The ingredient was heated to 930 °C at a rate of 50 °C min^{-1} while the base temperature was 880 °C under a constant pressure of 50 Pa for 20 min. 49 sccm Ar (5N) and 0.5 sccm O_2 (5N) were respectively used as carrier gases and oxygen source. After the reaction, other than automatically cooled

to room temperature, we took out reacted bases rapidly at 800 °C after the followed reaction temperature area. It is a spontaneous quenching process and without extra annealing process to activate Sb dopant source later, which is a crucial procedure for the LEDs performance. Finally, little margin of the post-reaction base was removed by diluted hydrochloric acid for Au sputtering, the Au were electric sputtered on n-GaN film at 10 Pa vacuum with 4 mA current for 60 s. Then, the In (5N) grain was placed on Au film and Sb-doped ZnO NWs, respectively. The In/p-ZnO Ohmic contact and In-Au/n-GaN Ohmic contact were formed after thermal annealing at 300 °C for 5min.

Characterization and Measurement: The morphologies, structure, and chemical composition of the samples were characterized by XRD (SHIMADZU XRD-7000), XPS (Kratos AXIS-ULTRA DLD-600W), high-resolution field emission SEM (FEI Nova Nano-SEM 450), TEM (FEI Titan G2 60–300). The analysis of electrical properties and luminescence performance at RT were characterized by IV (INTERLOCK IPD-12003SLU), EL (Avantes Avaspec-HS-TEC) and PL (Horiba JobinYvon LabRAM HR800), respectively. The EL and *I–V* characteristics of the devices were measured by applying a DC voltage to the device using a source meter (B2901A), carried through a two probe station. The EL spectra were measure by a high sensitivity fiber optic spectrometer equipped with a 1024 × 122 pixel TE cooled CCD detector (AvaSpec-HS1024×122TEC-USB2). The PL analysis down to 4.65 K was performed by the Ti:sapphire femtosecond laser (Coherent Mira 900) in superconducting magnet cryostat (OXFORD Microstat MO) and analyzed using monochromator (Shamrock 500i) with EMCCD (Newton 970) under the environment of liquid helium. The LEDs chromatogram was analyzed by CIE 1931 chromaticity diagram software (CIE1931xy. V1.6.0.2).

Supporting Information

Supporting Information is available from the Wiley Online Library or from the author.

Acknowledgements

X.R. and X.Z. contributed equally to this work. This work was supported by the National Basic Research Program (2011CB933300) of China, the National Natural Science Foundation of China (11374110, 11074082, 11204093, 51371085, 11304106). Y.G. would like to thank Prof. Zhong Lin Wang for the support of experimental facilities in WNLO of HUST.

Received: December 7, 2014
Revised: February 2, 2015
Published online: February 25, 2015

[1] N. Holonyak, S. F. Bevacqua, *Appl. Phys. Lett.* **1962**, *1*, 82.
[2] T. Jüstel, H. Niko, C. Ronda, *United States Patent* **2000**, *6*, 084, 250.
[3] D. A. Steigerwald, J. C. Bhat, D. Collins, R. M. Fletcher, M. O. Holcomb, M. J. Ludowise, P. S. Martin, S. L. Rudaz, *IEEE J. Sel. Top. Quant.* **2002**, *8*, 310.
[4] M. H. Crawford, *IEEE J. Sel. Top. Quant.* **2009**, *15*, 1028.
[5] F. A. Ponce, D. P. Bour, *Nature* **1997**, *386*, 351.
[6] H. Chen, *United States Patent* **1999**, *5*, 952, 681.
[7] J. K. Sheu, S. J. Chang, C. H. Kuo, Y. K. Su, L. W. Wu, Y. C. Lin, W. C. Lai, J. M. Tsai, G. C. Chi, R. K. Wu, *IEEE Photonic Tech L.* **2003**, *15*, 18.
[8] A. A. Setlur, A. M. Srivastava, H. A. Comanzo, D. D. Doxsee, *United States Patent* **2004**, *6*, 685, 852 B2.
[9] Y. Sun, N. C. Giebink, H. Kanno, B. Ma, M. E. Thompson, S. R. Forrest, *Nature* **2006**, *440*, 908.
[10] S. Reineke, F. Lindner, G. Schwartz, N. Seidler, K. Walzer, B. Lüssem, K. Leo, *Nature* **2009**, *459*, 234.
[11] M. Granström, O. Inganäs, *Appl. Phys. Lett.* **1996**, *68*, 147.
[12] M. N. Huda, Y. Yan, S. H. Wei, M. M. Al-Jassim, *Phys. Rev. B.* **2008**, *78*, 195204.
[13] X. H. Zhang, L. Y. Li, J. Su, Y. M. Wang, Y. L. Shi, X. L. Ren, N. S. Liu, A. Q. Zhang, J. Zhou, Y. H. Gao, *Laser Photon. Rev.* **2014**, *8*, 429.
[14] O. Lupan, T. Pauporté, B. Viana, *Adv. Mater.* **2010**, *22*, 3298.
[15] X. M. Zhang, M. Y. Lu, Y. Zhang, L. Chen, Z. L. Wang, *Adv. Mater.* **2009**, *21*, 2767.
[16] H. K. Fu, C. L. Cheng, C. H. Wang, T. Y. Lin, Y. F. Chen, *Adv. Funct. Mater.* **2009**, *19*, 3471.
[17] O. Lupan, T. Pauporté, T. L. Bahers, B. Viana, I. Ciofini, *Adv. Funct. Mater.* **2011**, *21*, 3564.
[18] O. Lupan, T. Pauporté, B. Viana, V. V. Ursaki, I. M. Tiginyanu, V. Sontea, L. Chow, *J. Nanoelectron. Optoelectron.* **2012**, *7*, 712.
[19] S. Limpijumnong, S. B. Zhang, S. H. Wei, C. H. Park, *Phys. Rev. Lett.* **2004**, *92*, 155504.
[20] S. Chu, G. P. Wang, W. H. Zhou, Y. Q. Lin, L. Chernyak, J. Z. Zhao, J. Y. Kong, L. Li, J. J. Ren, J. L. Liu, *Nat. Nanotechnol.* **2011**, *6*, 506.
[21] A. B. Yankovich, B. Puchala, F. Wang, J. H. Seo, D. Morgan, X. D. Wang, Z. Q. Ma, A. V. Kvit, P. M. Voyles, *Nano Lett.* **2012**, *12*, 1311.
[22] T. H. Kao, J. Y. Chen, C. H. Chiu, C. W. Huang, W. W. Wu, *Appl. Phys. Lett.* **2014**, *104*, 111909.
[23] L. L. Shi, F. Wang, B. H. Li, X. Chen, B. Yao, D. X. Zhao, D. Z. Shen, *J. Mater. Chem. C* **2014**, *2*, 5005.
[24] F. X. Xiu, Z. Yang, L. J. Mandalapu, D. T. Zhao, J. L. Liu, *Appl. Phys. Lett.* **2005**, *87*, 252102.
[25] J. Z. Zhao, H. W. Liang, J. C. Sun, J. M. Bian, Q. J. Feng, L. Z. Hu, H. Q. Zhang, X. P. Liang, Y. M. Luo, G. T. Du, *J. Phys. D Appl. Phys.* **2008**, *41*, 195110.
[26] E. V. Benvenutti, Y. Gushikem, A. Vasquez, S. C. Castroc, G. Zaldivar, *J. Chem. Soc., Chem. Commun.* **1991**, *19*, 1325.
[27] R. Delobel, H. Baussart, J. M. Lero, *J. Chem. Soc.* **1983**, *79*, 879.
[28] R. Izquierdo, E. Sacher, A. Yelon, *Appl. Surf. Sci.* **1989**, *40*, 175.
[29] H. B. Zeng, G. T. Duan, Y. Li, S. K. Yang, X. X. Xu, W. P. Cai, *Adv. Funct. Mater.* **2010**, *20*, 561.
[30] J. H. Lim, C. K. Kang, K. K. Kim, I. K. Park, D. K. Hwang, S. J. Park, *Adv. Mater.* **2006**, *18*, 2720.
[31] N. X. Sang, Tay Chuan Beng, T. Jie, E. A. Fitzgerald, C. S. Jin, *Phys. Status Solidi A* **2013**, *210*, 1618.
[32] S. B. Zhang, S. H. Wei, A. Zunger, *Phys. Rev. B.* **2001**, *63*, 075205.
[33] Ü. Özgür, Ya. I. Alivov, C. Liu, A. Teke, M. A. Reshchikov, S. Doan, V. Avrutin, S. J. Cho, H. Morkoç, *J. Appl. Phys.* **2005**, *98*, 041301.
[34] S. Xu, C. Xu, Y. Liu, Y. F. Hu, R. S. Yang, Q. Yang, J. H. Ryou, H. J. Kim, Z. Lochner, S. Choi, R. Dupuis, Z. L. Wang, *Adv. Mater.* **2010**, *22*, 4749.
[35] R. J. Xie, H. Naoto, S. Ken, Y. Yoshinobu, M. Mamoru, *Appl. Phys. Lett.* **2004**, *84*, 5404.